

## Tomographic test of Bell's inequality for a time-delocalized single photon

Milena D'Angelo,<sup>1</sup> Alessandro Zavatta,<sup>2</sup> Valentina Parigi,<sup>1,3</sup> and Marco Bellini<sup>1,2,\*</sup>

<sup>1</sup>*LENS, Via Nello Carrara 1, 50019 Sesto Fiorentino, Florence, Italy*

<sup>2</sup>*Istituto Nazionale di Ottica Applicata, Largo E. Fermi, 6, I-50125, Florence, Italy*

<sup>3</sup>*Department of Physics, University of Florence, I-50019 Sesto Fiorentino, Florence, Italy*

(Received 1 December 2005; revised manuscript received 6 September 2006; published 29 November 2006)

Time-domain balanced homodyne detection is performed on two well-separated temporal modes sharing a single photon. The reconstructed density matrix of the two-mode system is used to prove and quantify its entangled nature, while the Wigner function is employed for an innovative tomographic test of Bell's inequality based on the theoretical proposal by Banaszek and Wodkiewicz [Phys. Rev. Lett. **82**, 2009 (1999)]. Provided some auxiliary assumptions are made, a clear violation of the Banaszek-Bell inequality is found.

DOI: [10.1103/PhysRevA.74.052114](https://doi.org/10.1103/PhysRevA.74.052114)

PACS number(s): 03.65.Ud, 03.65.Wj, 03.67.Mn, 42.50.Dv

### I. INTRODUCTION

The concept of entanglement, as first introduced by Schrödinger [1] and discussed by Einstein, Podolsky, and Rosen [2] in 1935, has historically been associated with systems of two or more quanta. Its counterintuitive consequences found a mathematical formulation in the work of Bell [3] of 1964: pairs of quanta entangled in discrete variables (i.e., Bohm-like entangled systems [4]) may give rise to purely quantum nonlocal correlations. Unfortunately, no loophole-free test of Bell's inequality has been realized so far [5]. Besides their relevance in fundamental physics, these phenomena have attracted much attention due to their usefulness in quantum-information technology. Extravagant but promising protocols such as quantum teleportation, quantum cryptography, and quantum computation have been proposed and experimentally verified (see, e.g., [6] and references therein).

In the early 1990s, increasing attention has been given to a new perspective of quantum entanglement. The concept of entanglement has indeed been extended to any system containing a fixed number ( $N=1, 2, \dots$ ) of photons, provided at least one pair of spatiotemporal modes is involved. Then, even for  $N=1$ , one may talk of "single-photon  $n$ -mode entanglement," provided  $n \geq 2$ . The first steps in this direction were taken by Tan, Walls, and Collet [7] (TWC): when a single photon impinges on a beam splitter whose outputs are described by the spatial modes  $A$  and  $B$ , the emerging single photon is described by the state  $|\psi\rangle = \alpha|1\rangle_A|0\rangle_B + \beta|0\rangle_A|1\rangle_B$ , where  $|0\rangle$  is the vacuum,  $|1\rangle$  is a single-photon Fock state, and  $\alpha$  and  $\beta$  are complex amplitudes such that  $|\alpha|^2 + |\beta|^2 = 1$ . In this perspective, a single photon, with its presence or absence from a given spatiotemporal mode, may represent a tool for entangling two (or more) well-separated field modes. In this case, an experimental test of nonlocality would consist in performing simultaneous measurements on the separate field modes "sharing" the single photon and check if their mutual correlations violate a Bell's inequality.

Intensive studies and debates have been dedicated to the meaningfulness of extending both the concepts of entangle-

ment and nonlocality to TWC-type single-photon two-mode systems (see, e.g., [8–15]). Quite recently, Babichev *et al.* [11] and Zavatta *et al.* [14] have experimentally characterized a source of two-mode spatially and temporally delocalized single photons, respectively, by employing time-domain homodyne tomography [16] and reconstructing both density matrix and Wigner function of the measured system. In this respect, it is worth recalling that the density matrix or Wigner function of a given system represents its most complete characterization and enables predicting the result of any possible measurement one may perform on the system [17]. The results indicate the existence of strong correlations between the two spatial or temporal modes carrying a coherently delocalized single photon. Whether or not such correlations are nonlocal cannot be asserted; for instance, the Bell's inequality test performed in Ref. [11] is based upon dichotomization of quadrature data and heavily relies upon data rejection. Of particular interest, in this respect, is the experiment by Hessmo *et al.* [12], who have implemented the theoretical proposals by Tan *et al.* [7] and by Hardy [9], demonstrating the nonclassical character of the correlations characterizing two spatial modes sharing a single photon.

Similar to the two-photon case, also "entangled" single-photon sources may find immediate application in quantum-information technology: single-photon ebits have indeed been proven to enable linear optics quantum teleportation [18,19] and play a central role in linear-optics quantum computation [20,21]. Furthermore, the time-bin entanglement of the kind of Ref. [14] (see also [22,23]) has been proven suitable for long-distance applications [19,24], where the insensitivity to both depolarization and polarization fluctuations becomes a strong requirement.

In this paper, we wish to make one step further in the direction of understanding and proving single-photon  $N$ -mode entanglement. To this end, we employ the single-photon source presented in Ref. [14] (see Sec. III), perform two-mode homodyne tomography (Sec. IV), and employ the reconstructed two-mode density matrix and Wigner function to quantify the degree of entanglement (Sec. IV A) and implement an innovative kind of tomographic Bell's inequality test (Secs. II and IV B). In particular, we evaluate the degree of entanglement characterizing our single-photon system by employing Vidal and Werner's reformulation [25] of Peres separability criterion [26]. Then, we employ the ex-

\*Electronic address: bellini@inoa.it

perimentally reconstructed two-mode Wigner function to perform a continuous variable Bell's inequality test, based on the theoretical proposal by Banaszek and Wodkiewicz [10], which we briefly introduce in the next section.

## II. TOMOGRAPHIC TEST OF BELL'S INEQUALITY: BASIC IDEA

Let us start by briefly reviewing the theoretical proposal of Ref. [10]: the strict connection between the displaced parity operator (a dichotomic observable) and the Wigner function [16], suggests that the Wigner function of any two-mode or two-particle system (whether positive or negative) may play the role of a nonlocal correlation function. Bell's inequality can thus be recast in the form

$$|\mathcal{B}| = \frac{\pi^2}{4} |W(0,0) + W(\alpha_1,0) + W(0,\alpha_2) - W(\alpha_1,\alpha_2)| < 2, \quad (1)$$

where  $W(\alpha_1,\alpha_2)$  is the value of the two-mode Wigner function at the phase-space point  $(\alpha_1=x_1+iy_1, \alpha_2=x_2+iy_2)$  defined by the quadratures  $x_i$  and  $y_i$  of the  $i$ th mode or particle ( $i=1,2$ ). This inequality, which we shall name the Banaszek-Bell inequality, applies both to two-particle and to two-mode entangled systems, including spatially or temporally delocalized single photons. Interestingly, compared to all Bell's inequalities theoretically proposed for continuous variables and based upon *a posteriori* dichotomization of the measured field quadratures [27], the Banaszek-Bell inequality may achieve higher levels of violation. For instance, based on the predictions of quantum mechanics, the time-bin encoded single-photon state [14]

$$|\Psi\rangle = \frac{1}{\sqrt{2}}(|1\rangle_n|0\rangle_{n+1} + |0\rangle_n|1\rangle_{n+1}), \quad (2)$$

where  $n$  denotes a well-defined temporal mode (or time bin), is expected to maximally violate the inequality of Eq. (1), giving  $|\mathcal{B}| \approx 2.2$  for  $\alpha_1 = \alpha_2 \approx 0.3$ .

The experimental test of the Banaszek-Bell inequality, in the form written in Eq. (1), is feasible: our idea is to perform two-mode homodyne detection on the two distinct time bins ( $n$  and  $n+1$ ) carrying the temporally delocalized single photon of Eq. (2), and to use the experimental data to tomographically reconstruct the two-mode Wigner function entering the inequality of Eq. (1). Our ultrafast time-domain homodyne detection scheme has the potential to achieve this goal [28,29].

It is certainly true that, unlike the standard Bell's inequality tests, our tomographic test imposes an indirect approach to Bell's inequality: rather than directly employing the results of correlation measurements, our scheme requires the manipulation of the experimental quadrature data in order to reconstruct the Wigner function entering Eq. (1). Note, however, that the reconstruction procedure is rather transparent, does not imply additional hypotheses on the state under study, and can only introduce noise, without *hiding* or *enhancing* any information contained in the data. Then, finding

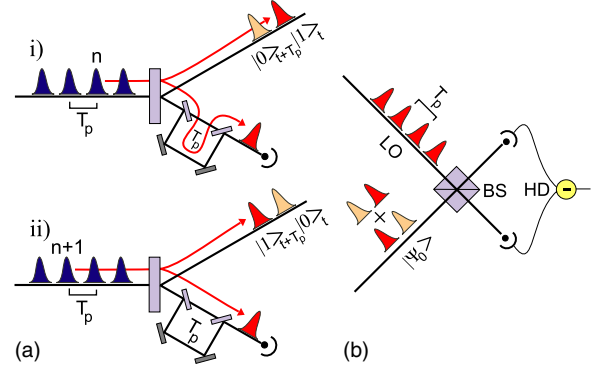


FIG. 1. (Color online) (a) Scheme for the remote preparation of a temporally delocalized single photon; (i) and (ii) indicate the two indistinguishable alternatives leading to the coherent superposition of Eq. (2) in the signal arm. (b) Scheme for the two-mode, time-domain, homodyne tomography of such a time-delocalized single-photon state.

a violation of Eq. (1) through a tomographic approach indicates that also direct measurements would lead to a violation.

## III. EXPERIMENTAL SETUP

Let us now consider the experimental setup: a mode-locked Ti:sapphire laser emitting 1.5 ps pulses at 786 nm at a repetition rate of 82 MHz, is frequency doubled in a lithium triborate (LBO) crystal; the resulting train of phase-locked pulses impinges on a nonlinear beta-barium borate (BBO) crystal, cut for degenerate noncollinear type-I spontaneous parametric down conversion [30]. Signal-idler photon pairs centered around 786 nm are generated in symmetric directions. Before entering an unbalanced fiber-based interferometer and being detected by a single-photon counter, the idler (trigger) photons undergo a narrow spectral and spatial selection aiming at the conditional generation of a pure single-photon state in the signal mode (see, e.g., [28,31]). Our setup is characterized by a single-photon preparation efficiency  $\eta_p=0.85$ , which depends on both the dark counts of the trigger detector and the purity of the prepared single photon [32]. The conditionally prepared signal beam impinges on a 50-50 beam splitter (BS) where it is mixed with a strong local oscillator (LO) made of an attenuated version of the train of laser pulses. Two-mode, high-frequency, time-domain, balanced homodyne detection is then performed on two consecutive signal pulses, as depicted in Fig. 1(b). The detection efficiency ( $\eta_d=0.74$ ) depends both on the efficiency of the two photodiodes ( $\eta_{PD}=0.88$ ) and optical losses, and on the mode matching with the local oscillator ( $\eta_{MM}=0.86$ ). The overall experimental efficiency of our setup is thus expected to be of the order of  $\eta=\eta_p\eta_d=0.63$ .

From the preparation viewpoint, the key part of our setup is the interferometer inserted in the idler channel: by setting the interferometer delay  $T$  equal to the fixed interpulse separation  $T_p$  characterizing the train of phase-locked pump pulses, a click in the idler channel does not distinguish the idler photon generated by the  $n$ th pump pulse which traveled the long arm, from the idler photon generated by the ( $n$

+1)th pump pulse which traveled the short arm [see Fig. 1(a)]. For an infinite train of mode-locked pump pulses and in the case of equal losses in the two arms of the interferometer, a click in the trigger detector projects the signal single photon onto the coherent superposition of Eq. (2).

#### IV. EXPERIMENTAL RESULTS

In order to check the degree of entanglement and to perform the tomographic test of Bell's inequality on such conditionally and remotely prepared temporally delocalized single photons, we have performed two-mode homodyne detection on the pair of consecutive signal time bins sharing the single photon; this is pictorially drawn in Fig. 1(b). By making use of what we have recently named "remote homodyne tomography" [14] to remotely vary the relative phase between the two-mode state and the LO pulses, we have performed about  $10^6$  quadrature measurements on the two consecutive signal temporal modes carrying the delocalized single photon. This has been made possible by the ultrafast operation of the homodyne detector recently developed in our laboratory [28,29].

The measured field quadratures have been employed to reconstruct the density matrix of the measured system by means of quantum tomography. In particular, we employ the pattern function (PF) method proposed by D'Ariano *et al.* [33] to directly retrieve the elements of the two-mode density matrix in the number-state base from the measured quadrature data:  $\rho_{klmn} = \langle k, l | \hat{\rho} | m, n \rangle$  is obtained from the statistical average of the corresponding pattern functions  $f_{km}(x, \theta)$  over all homodyne data, which is

$$\rho_{klmn} = \langle f_{km}(x_1, \theta_1) f_{ln}(x_2, \theta_2) \rangle_{x_1, \theta_1, x_2, \theta_2} \quad (3)$$

where  $x_{1,2}$  are the quadratures measured at phases  $\theta_{1,2}$  on the two consecutive time bins. The pattern functions have the form  $f_{km}(x, \theta) = F_{km}(x) e^{-i(m-k)\theta}$ , with  $F_{km}(x) = \partial [ \psi_k(x) \phi_m(x) ] / \partial x$  ( $m \geq k$ ), where  $\psi_k(x)$  and  $\phi_m(x)$  are, respectively, the regular and irregular wave functions of the harmonic oscillator [16,34]. In the experiment,  $\theta_2 - \theta_1$  is remotely varied by means of the interferometer while  $\theta_2 + \theta_1$  is left random since our system is independent of the global phase.

When reconstructing the quantum state, we allow each single-mode Fock state to contain from zero to two photons; each matrix index is thus varied from zero to two and a total of  $3^4 = 81$  density matrix elements are reconstructed for the two-mode system, as shown in Fig. 2(a). No assumptions are made on the system to be reconstructed; we just impose a truncation to the reconstruction space since no multiphoton contributions are expected.

The density matrix of the measured system has also been reconstructed by means of the maximum-likelihood (ML) method [35]: the density matrix  $\hat{\rho}$  that most likely represents the homodyne data is retrieved by maximizing a functional  $\mathcal{L}(\hat{\rho})$  involving the positive operator-valued measure associated with two-mode homodyne measurements. The only constraint we impose is that the density matrix  $\hat{\rho}$  is a positive-definite Hermitian matrix with unitary trace. In order to limit the number of free parameters in the minimization procedure,

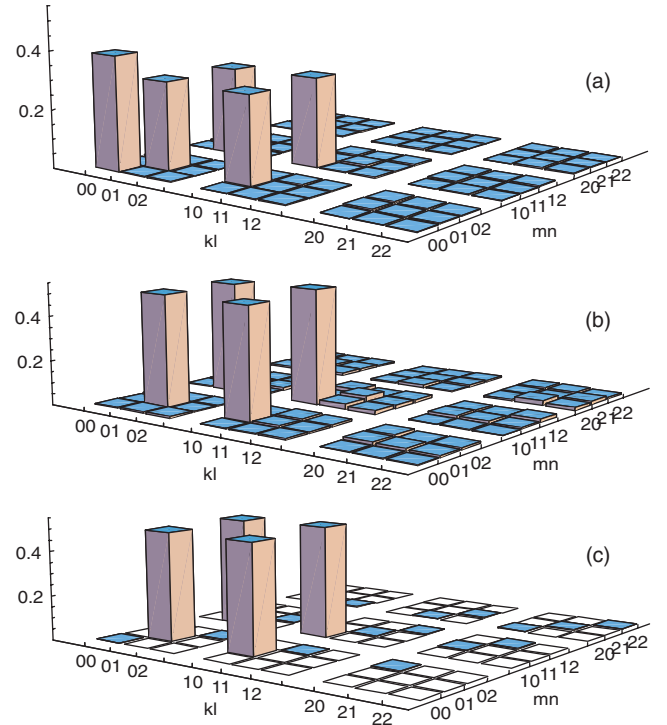


FIG. 2. (Color online) (a) Experimentally reconstructed density matrix elements (absolute values) relative to the mixed state of Eq. (4); (b) same elements after "vacuum cleaning" by an inverse Bernoulli transformation; (c) density matrix elements reconstructed with the maximum-likelihood method incorporating the experimental inefficiency.

we impose  $\hat{\rho}$  to be independent of the global phase  $\theta_2 + \theta_1$ . In principle, the ML method enables taking into account the experimental imperfections, thus reconstructing the density matrix of the measured system corrected for the experimental efficiency  $\eta$ . At this stage, we do not impose any such correction.

Both the PF and the ML methods (without correcting for  $\eta$ ) give very similar results; hence, in Fig. 2(a), we just plot the elements obtained from the PF method. The reconstructed density matrix contains both the expected state of Eq. (2) and a vacuum component ( $\rho_{0000}$ ) coming from the nonunitary experimental efficiency. The measured system is thus given by the mixture

$$\hat{\rho}_s = (1 - \eta) |0\rangle_{ss} \langle 0| + \eta |\Psi\rangle_{ss} \langle \Psi| \quad (4)$$

with  $|\Psi\rangle_s$  as given in Eq. (2); note that almost no multiphoton contribution exists in Fig. 2(a), as expected. From the vacuum component of the reconstructed density matrix we evaluate the overall efficiency to be  $\eta = 0.61$ , a result in good agreement with our estimated single-photon preparation and detection efficiencies.

#### A. Degree of entanglement

The reconstructed density matrix will now be employed to quantify the amount of entanglement characterizing the measured two-mode system. To this end, we use the logarithmic

negativity  $E_{\mathcal{N}}$  defined in [25], on the line of the Peres separability criterion [26]. In general, the Peres criterion gives a *necessary* condition for separability [26]: if a bipartite system is separable, the partial transpose of its density matrix (i.e., the transpose  $\hat{\rho}^{TA}$  of subsystem  $A$  alone) remains a physical density matrix with positive eigenvalues. Then, if we find that the partial transpose of our density matrix is not positive definite, we know our single-photon system is certainly nonseparable. In order to quantify the degree of nonseparability (i.e., the degree of entanglement), one can evaluate the logarithmic negativity defined as [25]:  $E_{\mathcal{N}}(\hat{\rho}) \equiv \log_2 \|\hat{\rho}^{TA}\|_1$ , where the symbol  $\|\cdot\|_1$  indicates the trace norm:  $\|\hat{\sigma}\|_1 \equiv \text{Tr} \sqrt{\hat{\sigma}^\dagger \hat{\sigma}}$ , which, for Hermitian matrices, reduces to  $\text{Tr} |\hat{\sigma}| = 1 + 2|\mathcal{N}|$ , with  $\mathcal{N}$  sum of the negative eigenvalues of  $\hat{\sigma}$  [25]. In other words, the trace norm accounts for the negative eigenvalues of  $\hat{\rho}^{TA}$ , and is thus directly related to the amount by which the partial transpose fails to be positive definite. In fact, for a separable system,  $\|\hat{\rho}^{TA}\|_1 = 1$  and the corresponding logarithmic negativity is zero; for a maximally entangled  $2 \times 2$  bipartite system,  $\|\hat{\rho}^{TA}\|_1 = 2$  and the corresponding logarithmic negativity is 1.

In our case, the reconstructed density matrix yields a logarithmic negativity  $E_{\mathcal{N}}(\hat{\rho}) = 0.404 \pm 0.001$ , thus showing the presence of some amount of entanglement even for non perfect detection efficiency. This result is perfectly in line with the value expected from Eq. (4), with  $\eta = 0.61$ . Interestingly, the bipartite system described by Eq. (4) is one of those “striking” mixtures which remain inseparable (i.e.,  $\hat{\rho}^{TA}$  has a negative eigenvalue) for any value of the efficiency  $\eta$  [26]. A coherently delocalized single photon is thus extremely robust against losses: its degree of entanglement may decrease but never vanishes.

### B. Test of Banaszek-Bell’s inequality

Based on the above result, our single-photon two-mode system is characterized by purely quantum correlations. Our next step is to check whether such quantum correlations are nonlocal. To this end, we reconstruct the two-mode Wigner function of the measured system [16]:

$$W(x_1, y_1; x_2, y_2) = \sum_{k,l,m,n} \rho_{klmn} W_{km}(x_1, y_1) W_{ln}(x_2, y_2) \quad (5)$$

where  $W_{ij}(x, y)$  is the Wigner function associated with the projector  $|i\rangle\langle j|$ , and  $\rho_{klmn}$  is the generic element of the experimentally reconstructed density matrix. The reconstructed Wigner function can now be used to evaluate the combination defined in Eq. (1), thus checking for a violation of the Banaszek-Bell inequality. We find that the parameter  $\mathcal{B}$  falls well within the limits imposed by local hidden-variable theories (see Fig. 3), a result that may be associated with the low overall experimental efficiency. In fact, in the case of limited

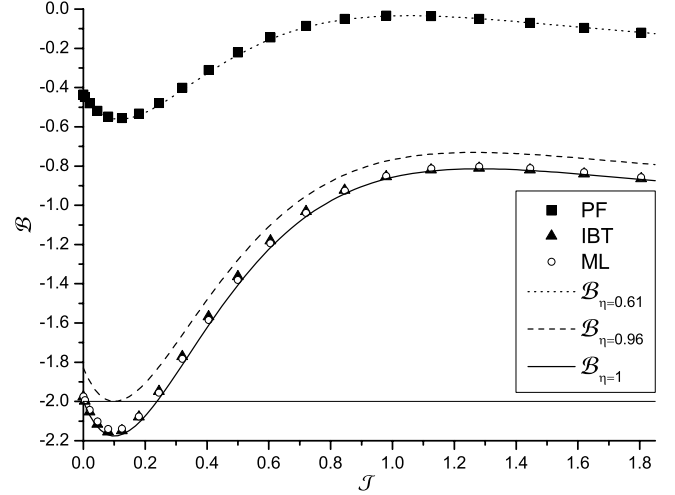


FIG. 3. Plot of the parameter  $\mathcal{B}_\eta(\mathcal{J})$  [Eq. (7)] for three different values of the overall efficiency  $\eta$ . Continuous curves are theoretical predictions, while the points come from the experimental data. The horizontal line indicates the lower bound imposed by the Banaszek-Bell inequality.

efficiency, the expected Wigner function for the state of Eq. (4) takes the form

$$W_\eta(\alpha_1, \alpha_2) = \frac{4[1 + 2\eta(|\alpha_1 + \alpha_2|^2 - 1)]}{\pi^2} e^{-2|\alpha_1|^2 - 2|\alpha_2|^2}; \quad (6)$$

hence, taking  $\alpha_1 = \alpha_2 = \sqrt{\mathcal{J}}$ , the combination given in Eq. (1) becomes

$$\mathcal{B}_\eta = 1 - 2\eta + e^{-2\mathcal{J}}[4\eta(\mathcal{J} - 1) + 2] - e^{-4\mathcal{J}}(8\mathcal{J}\eta - 2\eta + 1). \quad (7)$$

Its behavior is plotted in Fig. 3 as a function of the squared amplitude  $\mathcal{J}$  for different values of the global efficiency  $\eta$  and it is seen to closely match the experimental results (squared points) for  $\eta = 61\%$ . It is evident that the current level of experimental efficiency rules out the possibility of a loophole-free test of the Banaszek-Bell inequality, which would be attainable only for global experimental efficiencies larger than 96%.

To satisfy such strict requirements we need to introduce some auxiliary assumptions. In this perspective, it is worth noting that, different from photon counting, homodyne tomography allows one to explicitly *see* the effect of the experimental inefficiencies on the measured system: the overall efficiency  $\eta$  enters into the reconstructed density matrix [Fig. 2(a)] in the form of a vacuum. In particular, we find that the vacuum component remains exactly the same when no interferometer is inserted in the idler channel and a single signal photon is perfectly localized within a given temporal mode. This indicates that the nonunitary efficiency  $\eta$  represents our inability of producing and detecting a pure single-photon state, but, once such an imperfect single photon is coherently delocalized between separate time bins, the coherence is not further affected by losses. This is apparent from Fig. 2(a), where all the density matrix elements associated with the

entangled state of Eq. (2) have approximately equal weights. In other words, both detection and preparation inefficiencies give rise to state-independent losses as if a beam splitter with transmissivity  $\eta$  were introduced in the signal path, mixing vacuum with the original state [see Eq. (4) and Fig. 2(a)]. Correcting for our nonunitary efficiencies is thus similar to making the standard fair-sampling assumption [5].

Based on this reasoning, we have chosen to reconstruct the density matrix of the measured system by correcting for the nonunitary efficiency; this is expected to remove the vacuum component from the reconstructed density matrix, which is, to make the  $\rho_{0000}$  element almost equal to zero and rescale the other elements accordingly. We will implement such vacuum removal by employing two different strategies. The Banaszek-Bell inequality will thus be tested under the fair-sampling assumption or, more precisely, on the resulting “vacuum-cleaned” Wigner function.

In the first case, we account for losses by making an inverse Bernoulli transformation (IBT) of the reconstructed density matrix; the result is shown in Fig. 2(b). The basic idea is to model the nonperfect experimental efficiency by a beam splitter with transmissivity  $\eta$  followed by an ideal detector: the measured system  $\hat{\rho}_{\text{meas}}$  can be seen as the attenuated version of the system incident on such fictitious beam splitter. Since the output state of the beam splitter is related to the input state by a Bernoulli transformation, inversion of this transformation gives the state  $\hat{\rho}$  of the “incident” system, before its mixing with vacuum (i.e., before losses affect it) [36].

In the second case, we directly reconstruct the loss-free density matrix by adopting the maximum-likelihood (ML) method while taking into account the experimental efficiency  $\eta=0.61$ . The results are shown in Fig. 2(c) [37].

As shown in Fig. 3, the Wigner functions reconstructed from both the vacuum-cleaned density matrices give rise to a good agreement between the experimental data and the theoretical prediction of Eq. (7), with unitary efficiency. The temporally delocalized single photon thus clearly violates the lower bound of the Banaszek-Bell inequality under our version of the fair-sampling assumption.

Despite the observed violation of the Banaszek-Bell inequality, we cannot claim nonlocality for our single-photon time-encoded two-mode system. In fact, even in the case of unitary efficiency, our measuring scheme would still not satisfy the locality hypothesis: quadrature measurements on the two modes are actually done in sequence, so that a physical signal can in principle be exchanged between the two copropagating temporal modes while homodyne measurements are performed on them. The existence of this possibility makes our Bell's inequality test subject to the so-called locality loophole, which automatically rules out the possibility of claiming nonlocality [38]. However, this loophole simply derives from our choice of a temporal delocalization of the single photon and can in principle be eliminated in future experiments by introducing a fast switch which converts the two copropagating temporal modes into two spatially separated modes; simultaneous measurements could then be performed on each of the two time bins by two distant homodyne detectors.

## V. DISCUSSION AND CONCLUSIONS

Our results demonstrate the feasibility of the tomographic approach to Bell's inequality and may open the way toward new experiments for testing the foundations of quantum mechanics. Most important, our experiment sheds some light on the hotly debated concepts of single-photon two-mode entanglement and nonlocality [7–13,15]. On the one hand, single-photon two-mode states of the kind described by Eq. (2) are known to give rise to interference upon recombination of the two spatiotemporal modes through an interferometric scheme; in this perspective, the TWC entanglement between two spatial modes sharing a single photon can be visualized in terms of wave-particle duality: the interference upon recombination supports the wave picture of light, while the lack of coincidence counts at the two exits of the entrance beam splitter brings into evidence its particle nature. On the other hand, we have shown that our single-photon two-mode system manifests entanglement, both in terms of Peres-like separability criteria and, under additional hypotheses, in the more restrictive terms of Banaszek's version of Bell's inequality. The description of single-photon coherence effects in terms of single-photon  $N$ -mode entanglement is thus certainly possible and meaningful, and could contribute to make the counterintuitive wave-particle duality more intuitively accessible.

In summary, we have evaluated the degree of entanglement of a single photon coherently delocalized between two distinct temporal modes and have implemented an innovative test of Bell's inequality based on quantum homodyne tomography. We have shown that, within some auxiliary assumptions, the correlations between two well-separated temporal modes sharing a single photon violate the Banaszek-Bell inequality. In this respect, it is worth emphasizing that none of our additional hypotheses is, in principle, indispensable. In fact, different from Bell's tests relying on postselection, an improvement in the experimental efficiencies would allow us to avoid the fair-sampling assumption; indeed, a setup with an almost perfect single-photon preparation efficiency is currently possible. Furthermore, a slight modification of the experimental setup would easily eliminate the locality loophole. Thanks to the high efficiencies achievable by homodyne detectors, our tomographic approach may represent the first step in the direction of a loophole-free test of Bell's inequality. In this perspective, also the debated issue concerning the possibility of extending both concepts of entanglement and nonlocality to a coherently delocalized single photon, finds here an interesting preliminary answer.

## ACKNOWLEDGMENTS

This work has been performed in the frame of the “Spettroscopia laser e ottica quantistica” project of the Physics Department of the University of Florence and partially supported by Ente Cassa di Risparmio di Firenze and MIUR, under the PRIN initiative, and FIRB Contract No. RBNE01KZ94.

- [1] E. Schrödinger, *Naturwiss.* **23**, 807 (1935); **23**, 823 (1935); **23**, 844 (1935).
- [2] A. Einstein, B. Podolsky, and N. Rosen, *Phys. Rev.* **47**, 777 (1935).
- [3] J. S. Bell, *Physics* (Long Island City, N.Y.) **1**, 195 (1964).
- [4] D. Bohm, *Quantum Theory* (Prentice-Hall, Englewood Cliffs, NJ, 1951).
- [5] The most common auxiliary assumptions involved in the experimental tests of Bell's inequality are (1) the fair-sampling assumption, namely, the hypothesis that undetected events coming from low detection efficiencies would follow the same statistics of the measured data set, (2) postselection, which consists in disregarding part of the state of a physical system by not measuring it (i.e., imposing a selective, or state-dependent, loss mechanism), and (3) the locality loophole, which arises whenever a physical signal could be exchanged between the two systems under investigation during the measurement process.
- [6] C. H. Bennett *et al.*, *Nature* (London) **404**, 247 (2000).
- [7] S. M. Tan, D. F. Walls, and M. J. Collett, *Phys. Rev. Lett.* **66**, 252 (1991).
- [8] E. Santos, *Phys. Rev. Lett.* **68**, 894 (1992); L. Hardy, *ibid.* **75**, 2065 (1995), and references therein; D. M. Greenberger *et al.*, *ibid.* **75**, 2064 (1995); A. Peres, *ibid.* **74**, 4571 (1995); D. Home *et al.*, *Phys. Lett. A* **209**, 1 (1995); K. Jacobs and P. L. Knight, *Phys. Rev. A* **54**, R3738 (1996).
- [9] L. Hardy, *Phys. Rev. Lett.* **73**, 2279 (1994).
- [10] K. Banaszek and K. Wodkiewicz, *Phys. Rev. A* **58**, 4345 (1998); *Phys. Rev. Lett.* **82**, 2009 (1999).
- [11] S. A. Babichev *et al.*, *Phys. Rev. Lett.* **92**, 193601 (2004).
- [12] B. Hessmo, *et al.*, *Phys. Rev. Lett.* **92**, 180401 (2004).
- [13] S. J. Van Enk, *Phys. Rev. A* **72**, 064306 (2005).
- [14] A. Zavatta *et al.*, *Phys. Rev. Lett.* **96**, 020502 (2006).
- [15] M. Pawłowski and M. Czachor, [quant-ph/0507151](https://arxiv.org/abs/quant-ph/0507151), and *Phys. Rev. A* **73**, 042111 (2006).
- [16] U. Leonhardt, *Measuring the Quantum State of Light* (Cambridge University Press, Cambridge, 1997).
- [17] M. G. A. Paris and J. Rehacek (Eds.), *Quantum State Estimation* (Springer, Berlin, 2004).
- [18] S. Giacomini *et al.*, *Phys. Rev. A* **66**, 030302 (2002).
- [19] H. de Riedmatten *et al.*, *Phys. Rev. Lett.* **92**, 047904 (2004).
- [20] E. Knill *et al.*, *Nature* (London) **409**, 46 (2001).
- [21] T. B. Pittman *et al.*, *Phys. Rev. A* **71**, 032307 (2005).
- [22] J. Brendel *et al.*, *Phys. Rev. Lett.* **82**, 2594 (1999); H. de Riedmatten *et al.*, *Phys. Rev. A* **69**, 050304 (2004).
- [23] C. Simon *et al.*, *Phys. Rev. Lett.* **94**, 030502 (2005).
- [24] I. Marcikic *et al.*, *Nature* (London) **421**, 509 (2003).
- [25] G. Vidal and R. F. Werner, *Phys. Rev. A* **65**, 032314 (2002).
- [26] A. Peres, *Phys. Rev. Lett.* **77**, 1413 (1996).
- [27] B. Yurke *et al.*, *Phys. Rev. Lett.* **79**, 4941 (1997); J. Wenger *et al.*, *Phys. Rev. A* **67**, 012105 (2003); S. Daffer *et al.*, *ibid.* **72**, 034101 (2005).
- [28] A. Zavatta *et al.*, *Phys. Rev. A* **70**, 053821 (2004).
- [29] A. Zavatta *et al.*, *Science* **306**, 660 (2004); *Phys. Rev. A* **72**, 023820 (2005).
- [30] T. E. Keller and M. H. Rubin, *Phys. Rev. A* **56**, 1534 (1997); Y.-H. Kim *et al.*, *Phys. Rev. A* **62**, 043820 (2000).
- [31] A. I. Lvovsky *et al.*, *Phys. Rev. Lett.* **87**, 050402 (2001).
- [32] By defining the purity parameter as  $P = \text{Tr}(\hat{\rho}_s^2)$ , we get, in the spectral and the spatial domains, respectively:  $P_{\text{spectral}} = 1/\sqrt{1 + \Delta\omega_i^2/\Delta\omega_p^2} = .98$ , and  $P_{\text{spatial}} = 1/(1 + \Delta\kappa_i^2/\Delta\kappa_p^2) = 0.86$ , where Gaussian profiles with spectral and spatial widths  $\Delta\omega_j^2$  and  $\Delta\kappa_j^2$  are assumed both for the pump power spectrum ( $j = p$ ) and for the filter transmission function in the idler channel ( $j = i$ ). The contribution of purity to the single-photon preparation efficiency is  $\eta_{\text{purity}} = \sqrt{P_{\text{spectral}} P_{\text{spatial}}} = 0.92$ .
- [33] G. M. D'Ariano *et al.*, *Phys. Rev. A* **50**, 4298 (1994).
- [34] G. M. D'Ariano, in *Quantum Optics and Spectroscopy of Solids*, edited by T. Hakioglu and A. Shumovsky (Kluwer Academic, Dordrecht, 1997), pp. 175–202.
- [35] K. Banaszek *et al.*, *Phys. Rev. A* **61**, 010304(R) (1999).
- [36] T. Kiss *et al.*, *Phys. Rev. A* **52**, 2433 (1995).
- [37] After the vacuum-cleaning procedure, we find  $E_{\mathcal{N}}(\hat{\rho}) = 0.99 \pm 0.01$ , which is very close to the unitary value expected for the pure state of Eq. (2). The amount of entanglement required for observing a violation of the Banaszek-Bell inequality is  $E_{\mathcal{N}} > 0.942$ ; as far as the identification of entanglement is concerned, the more restrictive bounds imposed by Bell's inequality with respect to Peres criterion appear here explicitly.
- [38] In this respect, it is worth recalling that also the first historical Bell's inequality tests were affected by the locality loophole; the problem was solved for the first time by A. Aspect *et al.*, *Phys. Rev. Lett.* **49**, 1804 (1982).